



Nitrogen Doped Graphene: Influence of Precursors and Conditions of the Synthesis

Journal:	<i>Journal of Materials Chemistry C</i>
Manuscript ID:	TC-ART-11-2013-032359.R2
Article Type:	Paper
Date Submitted by the Author:	28-Jan-2014
Complete List of Authors:	Wang, Lu; Nanyang Technological University, Chemistry and Biological Chemistry Sofer, Zdenek; Institute of Chemical Technology, Prague, Department of Inorganic Chemistry Luxa, Jan; Institute of Chemical Technology Prague, Department of Inorganic Chemistry Pumera, Martin; Nanyang Technological University, Chemistry and Biological Chemistry

ARTICLE

Nitrogen Doped Graphene: Influence of Precursors and Conditions of the Synthesis

Cite this: DOI: 10.1039/x0xx00000x

Lu Wang,^[a] Zdeněk Sofer,^[b] Jan Luxa,^[b] Martin Pumera*^[a]

Received 00th January 2012,
Accepted 00th January 2012

DOI: 10.1039/x0xx00000x

www.rsc.org/

Heteroatoms doped graphenes, especially nitrogen doped graphenes, which have attracted much attention due to their remarkable performance as parts of lithium-ion batteries, advanced catalyst support, super capacitors and fuel cells. The performance of doped materials strongly depends on the level of doping. While the nitrogen doped graphenes are synthesized by various methods, the parameters influencing the level of doping are seldom studied. Here we prepare nitrogen doped graphene by exfoliation of different graphite oxide (i.e. Staudenmaier, Hofmann and Hummers) in ammonia atmosphere at various exfoliation temperatures (i.e. 600 °C, 800 °C and 1000 °C). We study the efficiency of nitrogen doping using characterization methods such as scanning electron microscope, Raman spectroscopy, combustile elemental analysis and X-ray photoelectron spectroscopy. We show that level of doping strongly depends on type of the starting graphite oxide. This has very important implication on the fabrication of doped graphenes and we suggest that the graphite oxide preparation route must be always considered when one performs heteroatom doping of graphenes via thermal exfoliation route. In addition, we present optimized, scalable technique for fabrication of large quantities of highly nitrogen doped (>7% at.) graphenes.

Introduction

Graphene is single layer of graphite, with carbon atoms covalently bonded in a hexagonal lattice. Due to this unique structure, graphene exhibits various interesting properties, such as high electrical conductivity, high thermal conductivity, good optical transparency, and large surface area.¹ Doping of heteroatoms such as boron² nitrogen,³⁻⁶ phosphorus,⁷ sulphur⁸, halogens^{9, 10} or hydrogen^{11, 12} can tailor the electronic and electrochemical properties of graphene, which can dramatically enhance the performance of doped graphene. Nitrogen doped graphene has attracted much attention due to its remarkable performance as parts of lithium-ion batteries,^{5,6} advanced catalyst support,¹³ super capacitors¹⁴ and fuel cells.³⁻⁵ The level of doping is of high importance as carrier density is crucial for tuning the performance of the material. Even though properties of N-doped graphene strongly depend on the concentration of dopant, limited number of studies actually investigate the variables influencing the level of doping.

There are different approaches of doping of graphene with heteroatoms. Some approaches are based on simply mixing graphene materials with nitrogen containing precursor (i.e. melamine) and carbonize mixture.¹⁵ Nitrogen doping can be also achieved by thermal exfoliation of graphite oxide in ammonia atmosphere.^{16,17} Solvent-based were tested by using graphene oxide and shift base precursors, leading to N-doped graphene.¹⁸ Amount of nitrogen introduced to the graphene lattice has been reported typically in range of 2-4 at %.^{4,5,13} The only methods capable of introduction larger amounts, of 9-11% at. are CVD based methods.^{6,14}

Here we present a study of the effects of level nitrogen doping by using different precursors and condition. We employ the scalable method capable of production of gram quantities of doped material via oxidative treatment of graphite to graphite oxide and consequent thermal exfoliation in NH₃ atmosphere. We vary parameters such as starting material preparation method (permanganate vs. chlorate based oxidation of graphite to graphite oxide; such materials exhibit very different

structural characteristics,¹⁹ even though they have similar C/O ratio) and temperature of exfoliation in NH₃ atmosphere. We will show that starting material preparation method have profound influence on doping levels of N-doped graphene. The influence of the condition used will be investigated by detailed characterization using scanning electron microscope, Raman spectroscopy, and X-ray photoelectron spectroscopy, as well as combustible elemental analysis. We show that by optimization of the synthetic conditions, it is possible to achieve doping over 7% at. nitrogen in graphene lattice.

Results and discussion

The precursors of N-doped graphenes were graphite oxides (GO) which were synthesized using chlorate oxidants (Staudenmaier and Hofmann methods)^{20,21} and permanganate oxidant (Hummers method).²² The nitrogen doped graphenes were prepared by thermally exfoliation of graphite oxides in ammonia atmosphere. The influence of starting graphite oxide type as well as of exfoliation temperature on the nitrogen doping and density of defects was studied. The control experiments were carried by exfoliation of GO in N₂ atmosphere. The N-doped graphenes are labelled in the following text by method of precursor synthesis (Staudenmaier (ST), Hofmann (HO), Hummers (HU)), by exfoliation temperature and by suffix “N” in case of exfoliation in NH₃ atmosphere (e.g. “ST-600-N”). For control materials exfoliated in N₂ atmosphere, suffix “N” is not used.

MORPHOLOGY. The morphology of all reduced graphene samples was investigated by SEM. Figure 1 shows the SEM images of different types of nitrogen doped graphenes which were obtained at magnification of 3000× and 20,000×. SEM images for control (N₂ atmosphere exfoliated) graphene are shown in the Support Information (SI), Figure S1. All materials showed a typical exfoliated structure in agreement with previous studies and confirmed successful thermal exfoliation of all types of graphite oxide samples in NH₃ atmosphere. We have also recorded XRD to provide full characterization of resulting N-doped materials (Figure S2, Supporting Information).

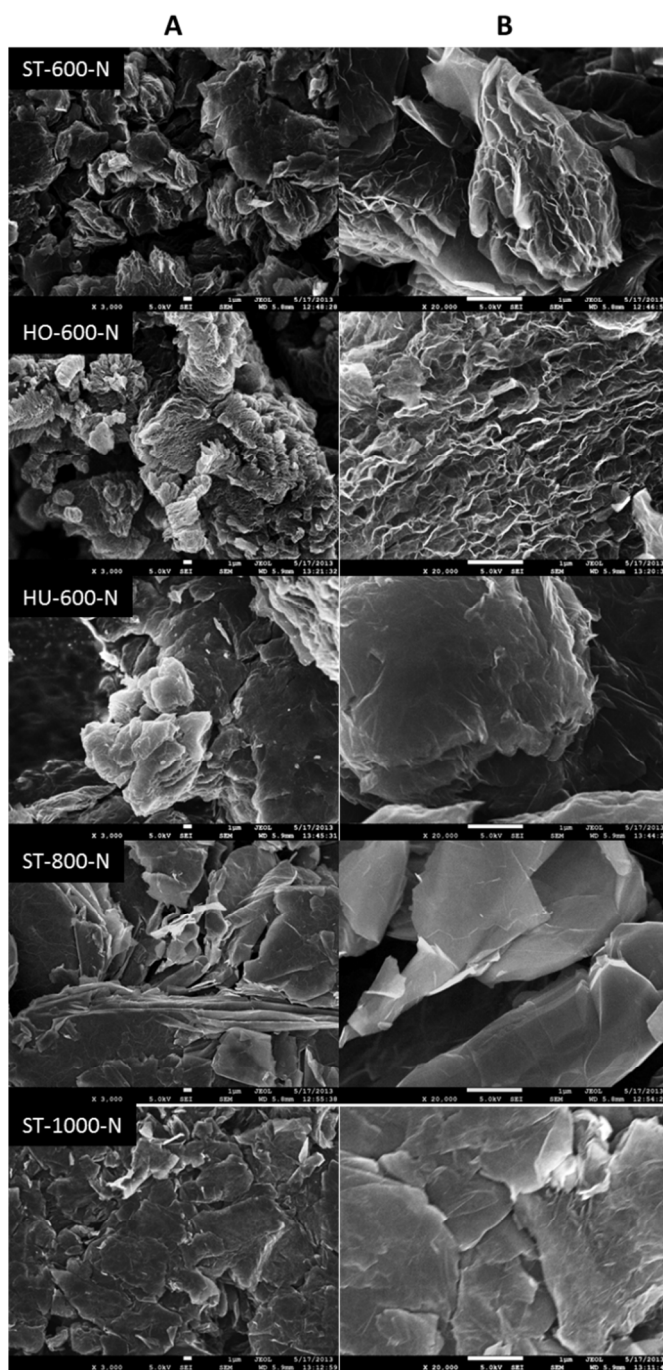


Figure 1. Scanning electron micrographs of nitrogen doped graphenes prepared by Staudenmaier (ST) graphite oxide at 600 °C, 800 °C and 1000 °C, Hofmann (HO) graphite oxide at 600 °C, and Hummers (HU) graphite oxide at 600 °C. Magnification of (A) 3000x and (B) 20,000x. Scale bar of 1µm.

RAMAN SPECTROSCOPY was used in order to determine the defect density of nitrogen doped graphene that prepared by different methods and different temperatures. Figure 2 show the Raman spectra and I_D/I_G ratio for the nitrogen doped graphene prepared by different methods and conditions. The G band at approximately 1560 cm⁻¹ indicates the presence of sp² lattice carbon atoms in the graphene sheet and a D band at approximately 1350 cm⁻¹ represents the defects caused by the

sp^3 hybridized carbon atoms, which is, as we will show later, related to doping of nitrogen atoms.

The ratio between D and G band intensities (I_D/I_G) is used to indicate the degree of disorder in a carbon structure. I_D/I_G ratio for ST-600-N, HO-600-N, HU-600-N increases from 0.89 to 0.95 and to 1.02, respectively. This indicates that the highest density of defects can be found in HU-600-N while lowest density of defects in ST-600-N. This reflects the fact that the graphite oxides are very different materials which undergo exfoliation via different routes, as shown previously.^{23, 24} Interestingly, increasing temperature of exfoliation from 600 °C to 1000 °C did not lead to monotonic trend; ST-600-N, ST-800-N, and ST-1000-N displayed I_D/I_G of 0.89, 0.41 and 0.77 respectively as shown in the bar chart in Figure 2.

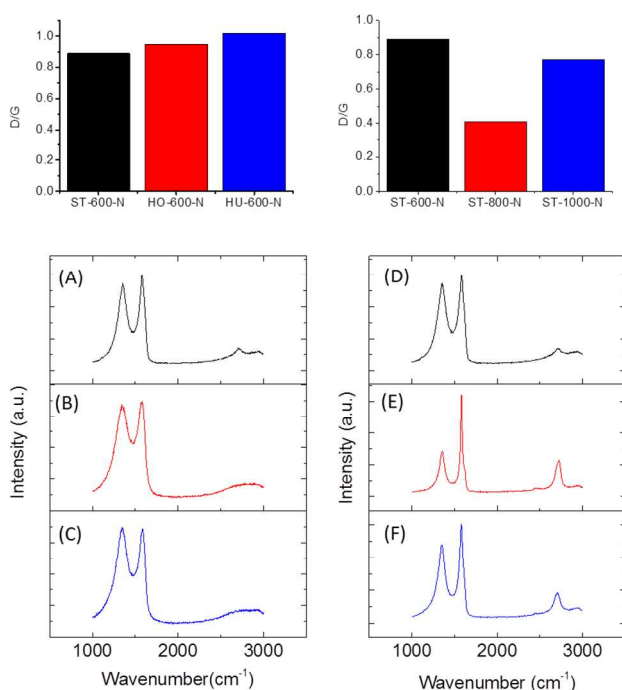


Figure 2. Left: I_D/I_G ratio and Raman spectra for nitrogen doped graphenes prepared by (A) Staudenmaier (ST) graphite oxide, (B) Hofmann (HO) graphite oxide, and (C) Hummers (HU) graphite oxide at 600 °C. Right: I_D/I_G ratio and Raman spectra for nitrogen doped graphenes prepared by Staudenmaier (ST) graphite oxide at (D) 600 °C, (E) 800 °C, and (F) 1000 °C.

Among the graphene prepared at 600 °C, only the ST-600-N exhibits a 2D band at approximately 2700 cm^{-1} , which indicate a lower degree of disorder in its carbon structure than HU-600-N and HO-600-N. In fact, all Raman spectrum of nitrogen doped graphene that prepared by ST graphite oxide at different temperature show a 2D band at approximately 2700 cm^{-1} indicating that all three nitrogen doped ST graphenes have a lower disorder structure when compared to other two graphite oxides.

The average crystallite sizes (L_a) of the various materials can be calculated based on the D and G band intensities by application of the Eq 1.²⁵

$$L_a = 2.4 \times 10^{-10} \times \lambda_{laser}^4 \times I_G/I_D \quad (1)$$

where λ_{laser} is the wavelength of the excitation laser in nanometres, and I_G and I_D are the intensities of the Raman G and D bands, respectively. Then we calculated the crystallite sizes in nitrogen doped graphene samples. We found that the L_a of ST-600-N, HO-600-N, HU-600-N, ST-800-N and ST-1000-N are 14.97 nm, 15.98 nm, 17.15 nm, 6.90 nm and 12.95 nm, respectively. Raman spectra of control graphene materials (exfoliated in N_2 atmosphere) are shown in Figure S3 (SI).

X-RAY PHOTOELECTRON SPECTROSCOPY. The elemental composition of nitrogen doped graphene samples were investigated by using XPS. The XPS can obtain not only the elemental composition, but also bonding information for selected elements. The wide scan, and C1s and N1s high-resolution XPS were obtained for all doped graphene samples and shown in Figure 3, 4 and 5 (corresponding XPS spectra of undoped graphene materials exfoliated in inert gas atmosphere are shown in Figures S4, S5 (SI)). The wide scan and high resolution XPS of C1s shown in Figure 3 and 4 for all nitrogen doped graphenes indicate that the oxygen containing groups were mostly removed, the thermally reduced graphenes were prepared successfully, and the nitrogen was successfully introduced into the graphene lattice. No nitrogen was observed in control (undoped) graphene samples prepared by exfoliation in N_2 atmosphere.

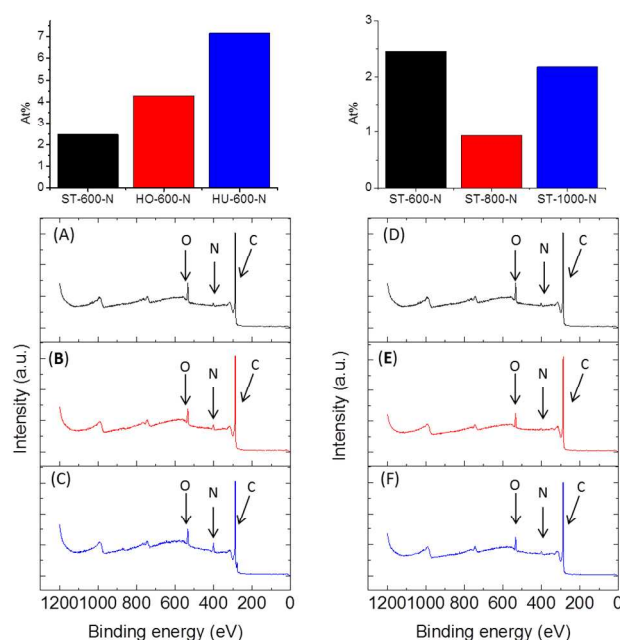


Figure 3. Left: N content and wide scan XPS for nitrogen doped graphenes prepared by (A) Staudenmaier (ST) graphite oxide, (B) Hofmann (HO) graphite oxide, and (C) Hummers (HU) graphite oxide at 600 °C. Right: N content and wide scan XPS for nitrogen doped graphenes prepared by Staudenmaier (ST) graphite oxide at (D) 600 °C, (E) 800 °C, and (F) 1000 °C.

The C/O ratio for ST-600-N, HO-600-N and HU-600-N are 11.6, 12.1 and 11.8 respectively, indicating that thermal reduction of graphite oxides was successfully achieved. The nitrogen content for different precursors increases in the row ST-600-N, HO-600-N and HU-600-N from 2.5 at%, 4.3 at% to

7.2 at%, respectively (Figure 3). It is apparent that the nitrogen doped graphene prepared from Hummers graphite oxide contains the largest amount of nitrogen; on contrary, the Staudenmaier graphite oxide as precursor leads to the lowest amount of nitrogen doping. It is noteworthy that density of defects (I_D/I_G ratio) exhibits the same trend as nitrogen content and appears to be closely related.

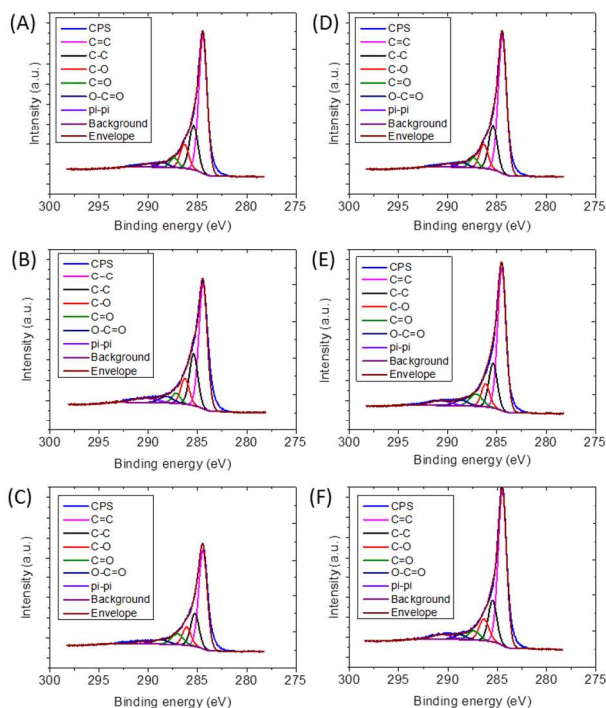


Figure 4. Left: High resolution XPS of C1s of nitrogen doped graphenes prepared by (A) Staudenmaier (ST) graphite oxide, (B) Hofmann (HO) graphite oxide, and (C) Hummers (HU) graphite oxide at 600 °C. Right: High resolution XPS of C1s of nitrogen doped graphenes prepared by Staudenmaier (ST) graphite oxide at (D) 600 °C, (E) 800 °C, and (F) 1000 °C.

Consequently, we have studied the influence of exfoliation temperature on the N content and the reduction of GO. C/O ratio of ST-600-N, ST-800-N and ST-1000-N are 11.6, 15.1 and 15.5 which show an increasing trend towards increasing exfoliation temperature. ST-600-N, ST-800-N and ST-1000-N contained 2.5 at%, 0.94 at% and 2.18 at% of nitrogen, respectively. There is no clear monotonic trend for amount of doped nitrogen along the exfoliation temperature. However, similar to the influence of the precursors study, the I_D/I_G ratio was closely related to nitrogen doping levels. The XPS data are consistent with nitrogen determination by combustible elemental analysis, as shown in Table 1.

Table 1. Combustible elemental analysis of N-doped graphene.

Sample	at. % N	at. % C	at. % H	at. % O
ST-600-N	2.25	90.03	1.09	6.63
HO-600-N	4.22	82.51	3.25	10.02
HU-600-N	6.86	76.46	7.35	9.33
ST-800-N	2.3	90.56	1.56	5.58
ST-1000-N	1.94	90.03	2.27	5.76

The high resolution XPS of C1s signal provides the insight into the chemical composition of residual oxygen containing groups, as they show different energy levels, C=C bond of 284.5 eV, C-C bond of 285.4 eV, C-O bond of 286.3 eV, C=O bond of 287.4 eV, O-C=O bond of 288.5 eV and π - π interactions of 290 eV. The detailed bonding information for all nitrogen doped graphenes is shown in Table 2. The high resolution XPS of N1s for nitrogen doped graphenes are shown in Figure 5. Similar to high resolution C1s, high resolution XPS of N1s signal shows the chemical composition at different energy levels; pyridine-like N bond at 397.9 eV, pyrrole-like N bond at 399.1 eV and Quaternary N at 401.3 eV. In precursors study, the ST-600-N, HO-600-N and HU-600-N contain 48.6 at %, 38.8 at % and 46.1 at % of pyridine-like N bond, 27.6 %, 14.5 % and 40.6 % of pyrrole-like N bond, and 23.8 at %, 46.6 at % and 13.3 at % of quaternary N bond respectively. In temperature study, the ST-600-N, ST-800-N and ST-1000-N contain 48.6 at %, 41.2 at % and 42.3 at % of pyridine-like N bond, 27.6 at %, 28.4 at % and 10.5 at % of pyrrole-like N bond, 23.8 at %, 30.4 at % and 47.1 at % of quaternary N bond respectively.

Table 2. Bonding arrangement in doped graphenes (%) from high resolution C1s XPS for all nitrogen doped graphene samples.

	C=C	C-C	C-O	C=O	O-C=O	π - π
HU-600-N	56.0	18.5	10.2	8.5	2.1	2.1
HO-600-N	53.0	21.9	10.8	4.2	4.5	5.4
ST-600-N	60.3	19.7	10.6	4.2	2.7	2.4
ST-800-N	61.7	12.6	15.1	5.5	3.9	1.1
ST-1000-N	57.2	17.8	9.1	7.4	3.7	4.8

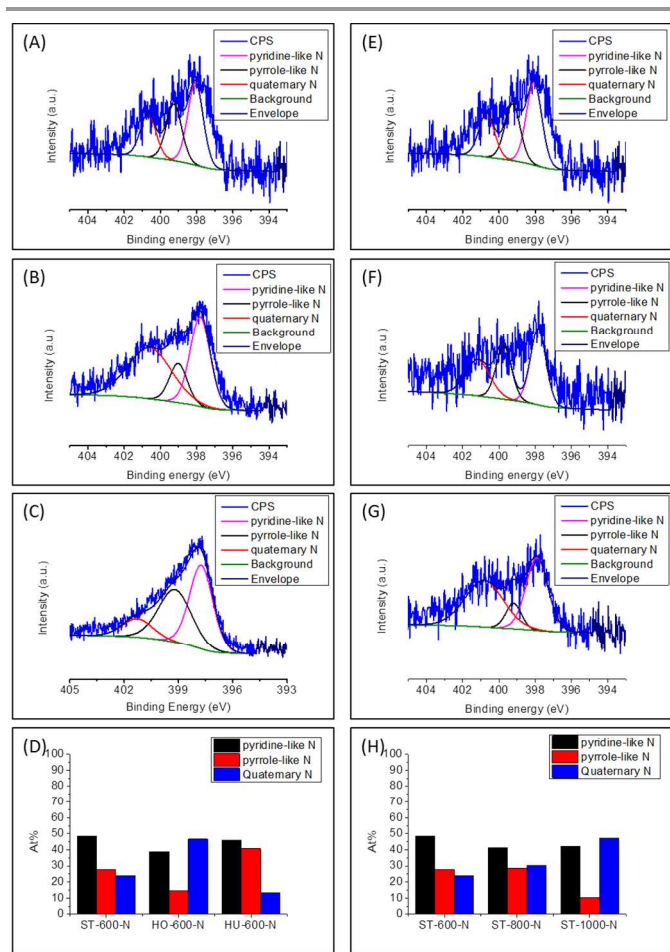


Figure 5. Left: high resolution XPS of N1s of nitrogen doped graphenes prepared by (A) Staudenmaier (ST) graphite oxide, (B) Hofmann (HO) graphite oxide, (C) Hummers (HU) graphite oxide at 600 °C, and (D) the bar chart of the nitrogen bonding information for nitrogen doped graphenes. Right: high resolution XPS of N1s of nitrogen doped graphenes prepared by Staudenmaier (ST) graphite oxide at (E) 600 °C, (F) 800 °C, (G) 1000 °C and (H) the bar chart of the nitrogen bonding information for nitrogen doped graphenes.

From specific resistivity measurements (4-point method), it can be seen that specific resistivity of the material is directly related to the nitrogen doping levels; as it can be seen in Table 3, when we compare three graphenes prepared by different methods at the same temperature, HU-600-N with 7.2at% of N shows the highest resistivity while the lowest amount of nitrogen doping in ST-600-N the lowest resistivity. As it can be observed, there is higher resistivity at high nitrogen concentrations due to the fact that increase of pyrrole-like N and quaternary nitrogen moieties increase of defect concentration which act as a scattering centres of free carriers. In addition, quaternary nitrogen creates p-doping site, effectively withdrawing electrons. When we look at relation of conductivities based on graphene prepared by Staudenmaier method at different temperatures, there is not clear dependency as varied density of defects may influence the conductivity as well. Resistivity of graphenes exfoliated in the inert atmosphere (un-doped) are stated in Table S1 (SI).

Table 3. Specific resistivity of N-doped graphenes.

Sample	Specific resistivity (Ohm.cm)
ST-600-N	5.6×10^{-5}
HO-600-N	2.3×10^{-4}
HU-600-N	1.7×10^{-3}
ST-800-N	2.6×10^{-4}
ST-1000-N	3.5×10^{-5}

Conclusions

It was found that type of precursor, such as type of graphite oxide used for preparation of the nitrogen-doped graphene, has major influence on level of doping. This is major contribution to the field since graphite oxides prepared by chlorate or permanganate routes are typically treated as interchangeable. Our findings on nitrogen doped graphenes confirm previous observations on sulphur doped graphenes, where similar trend related to preparation route of graphite oxide was observed.⁸ This is due to the differences in the structures of graphite oxide prepared by different methods. Among three types of precursors, Staudenmaier graphite oxide, Hofmann graphite oxide and Hummers graphite oxide, under same condition, the Hummers graphite oxide can be doped with the highest amount of nitrogen (7.2 % at) and the Staudenmaier graphite oxide can be doped the least amount of nitrogen (0.94 % at.). Therefore, we strongly suggest that type of used graphite oxide for preparation of doped graphenes shall be always considered as important variable.

Acknowledgements

M.P. acknowledges Tier 2 grant (MOE2013-T2-1-056; ARC 35/13) from Ministry of Education, Singapore. Z.S. and J.L. were supported by Specific University Research grant (MSMT No 20/2013).

Notes and references

^a L. Wang, Prof. M. Pumera
Division of Chemistry & Biological Chemistry
School of Physical and Mathematical Sciences
Nanyang Technological University
Singapore 637371
Fax: (65) 6791-1961
E-mail: pumera@ntu.edu.sg; pumera.research@outlook.com

^b Prof. Z. Sofer, J. Luxa
Institute of Chemical Technology,
Department of Inorganic Chemistry,
Technická 5, 166 28 Prague 6,
Czech Republic

Experimental

Materials

Graphite microparticles (<50 μm) was obtained from KOH-I-NOOR GRAFIT, Czech Republic. Sulfuric acid (96%), nitric acid (65%), nitric acid (fuming, >98%), potassium chlorate (98%), potassium permanganate (98%), hydrogen peroxide (30%), hydrochloric acid (35%), silver nitrate (99.8%) and barium nitrate (99 %) were obtained from PENTA, Czech Republic. Nitrogen gas (99.9999%) and Ammonia (99.9995%) was obtained from SIAD. *N,N*-dimethylformamide (DMF), potassium phosphate dibasic, and sodium phosphate monobasic were purchased from Sigma-Aldrich.

Apparatus

The scanning electron microscopy (SEM) images were obtained by a JEOL 7600F field emission scanning electron microscopy (JEOL, Japan). The Raman spectra were obtained by a confocal micro-Raman LabRam HR instrument from Horiba Scientific in backscattering geometry with a CCD detector. A 514.5nm Ar laser and a 100 \times objective lens were mounted on an Olympus optical. The calibration is made by using a silicon reference with a peak position at 520 cm^{-1} and a resolution less than 1 cm^{-1} . X-ray photoelectron spectroscopy (XPS) samples were prepared by compacting a uniform layer of the materials on a carbon tape. The XPS samples were measured by a monochromatic Mg X-ray radiation source (SPECS, Germany) and a Phoibos 100 spectrometer in order to obtain survey and high resolution C1s, O1s and N1s spectra.

The combustible elemental analysis was performed with CHN PE 2400 Series II from Perkin Elmer (USA). In CHN operating mode (the most robust and interference free mode), the instrument employs a classical combustion principle to convert the sample elements to simple gases (CO_2 , H_2O and N_2). The PE 2400 analyzer performs automatically combustion and reduction, homogenization of product gases, separation and detection. A microbalance MX5 (Mettler Toledo) is used for precise weighing of samples (1.5 – 2.5 mg per single sample analysis). The accuracy of CHN determination is better than 0.30% abs. Internal calibration was performed using *N*-phenyl urea.

Specific resistivities of MVGs were measured by first compressing 40 mg each of the materials into a capsule (diameter 63.5 mm) under a pressure of 400 MPa for 30 s. The resistivity of the resulting capsule was then measured according to the van der Pauw method²⁶ with a 4-probe technique, using a home-made system with a Keithley 6220 current source and an Agilent 34970A data acquisition/switch unit.

X-ray powder diffraction data were collected at room temperature with an X'Pert PRO θ - θ powder diffractometer with parafocusing Bragg-Brentano geometry using $\text{CuK}\alpha$ radiation ($\lambda = 1.5418 \text{ \AA}$, $U = 40 \text{ kV}$, $I = 30 \text{ mA}$). Data were scanned with an ultrafast detector X'Celerator over the angular range 5-80 $^\circ$ (2θ) with a step size of 0.0167 $^\circ$ (2θ) and a counting time of 20.32 s step^{-1} . Data evaluation was performed in the software package HighScore Plus.

Graphite oxide preparation with the Staudenmaier method.

87.5 mL of sulfuric acid (96% concentration) and 27 mL of fuming nitric acid were added to a reaction flask which contains a magnetic stir bar. The mixture was subsequently cooled by immersion in an ice bath for 30 min. Then 5 g of graphite was added into the mixture with vigorous stirring motion to acid agglomeration and obtain a homogeneous dispersion. 55 g of potassium chlorate was slowly added to the mixture (over a 30 min period) while the reaction flask in an ice bath to avoid a sudden increment in temperature and formation of explosive chlorine dioxide gas. When potassium chlorate was completely dissolved, the reaction flask was loosely capped to allow the evolved gas to escape and the mixture was continuously stirred vigorously for 96 h at temperature. When reaction was finished, the mixture was poured into 3 L of deionized water and decanted. In order to remove sulfate ions, graphite oxide was then redispersed in HCl (5%) solution and repeatedly centrifuged and redispersed in deionized (DI) water until negative reaction on chloride and sulfate ions (with AgNO_3 and $\text{Ba(NO}_3)_2$ respectively) was achieved. Then the graphite oxide slurry was dried in a vacuum oven at 60 $^\circ\text{C}$ for 48 h before use.

Graphite oxide preparation with the Hofmann method.

27 mL of nitric acid (65%) and 87.5 mL of sulfuric acid (96%) were added to a reaction flask (Pyrex beaker with thermometer) which contains a magnetic stir bar and the mixture was then cooled by immersion in an ice bath for 30 min. In order to avoid agglomeration and obtain a homogeneous dispersion, 5 g of graphite was added to the mixture with vigorous stirring motion. 55 g of potassium chlorate was slowly added to the mixture (over a 30 min period) while the reaction flask in an ice bath to avoid a sudden increment in temperature and formation of explosive chlorine dioxide gas. When potassium chlorate was completely dissolved, the reaction flask was loosely capped to allow the evolved gas to escape and the mixture was continuously stirred vigorously for 96 h at temperature. When reaction was finished, the mixture was poured into 3 L of

deionized water and decanted. In order to remove sulfate ions, graphite oxide was then redispersed in HCl (5%) solution and repeatedly centrifuged and redispersed in deionized (DI) water until negative reaction on chloride and sulfate ions (with AgNO_3 and $\text{Ba(NO}_3)_2$ respectively) was achieved. Then the graphite oxide slurry was dried in a vacuum oven at 60 $^\circ\text{C}$ for 48 h before use.

Graphite oxide preparation with the Hummers method.

2.5 g of sodium nitrate and 5 g of graphite were stirred with 115 mL of sulfuric acid (98%) and the mixture was cooled in an ice bath. 15 g of potassium permanganate was added with vigorous stirring over two hours. In following 4 hours, the mixture was allowed to reach room temperature before being heated to 35 $^\circ\text{C}$ for 30 min. Then the mixture was poured into a flask which contains 250 mL of DI water and further heated to 70 $^\circ\text{C}$. The temperature of mixture was held constantly for 15 min and poured into 1 L of DI water. Hydrogen peroxide (3%) was added to remove unreacted manganese dioxide and potassium permanganate. Then the mixture was allowed to settle and decanted. The formed graphite oxide was purified by repeated centrifugation and redispersing in DI water until a negative reaction on sulfate ion (with $\text{Ba(NO}_3)_2$) was achieved. Then the graphite oxide slurry was dried in a vacuum oven at 60 $^\circ\text{C}$ for 48 h before use.

Thermally reduced graphenes.

Thermally reduced graphenes (TR-G) were formed by thermal exfoliation/reduction of graphite oxides at 600 $^\circ\text{C}$ and 1000 $^\circ\text{C}$. 0.1 g of graphite oxide was placed into a porous quartz glass capsule which connects to a magnetic manipulator and placed inside a vacuum tight tube furnace with a controlled atmosphere. The magnetic manipulator is able to create a temperature gradient over 1000 $^\circ\text{C min}^{-1}$. In order to remove oxygen, the sample was flushed with nitrogen gas by repeated evacuation of the tube furnace. Then the sample was inserted by the magnetic manipulator to a preheated furnace and held in the furnace for 12 min. The flow of nitrogen (99.9999%) during the exfoliation procedure was 1000 mL min^{-1} to remove any byproducts from the procedure.

Synthesis of N doped graphene.

The nitrogen doped graphene was prepared by exfoliation of produced graphite oxide in ammonia atmosphere. 100 mg of graphite oxide were placed inside the quartz glass capsule connected to the magnetic manipulator and placed in the horizontal quartz glass reactor. The reactor was repeatedly evacuated and flushed with nitrogen before the insertion of the sample within the hot zone. Subsequently the sample was inserted in the hot zone of the reactor and the nitrogen flow was switched to ammonia. The temperature of samples was held constantly for 12 min at 600 $^\circ\text{C}$, 800 $^\circ\text{C}$ and 1000 $^\circ\text{C}$. The ammonia with flow rate of 300 mL/min was used in order to remove the exfoliation byproducts.

Electronic Supplementary Information (ESI) available: [SEM, XRD, Raman spectra, XPS spectra of control materials]. See DOI: 10.1039/b000000x/

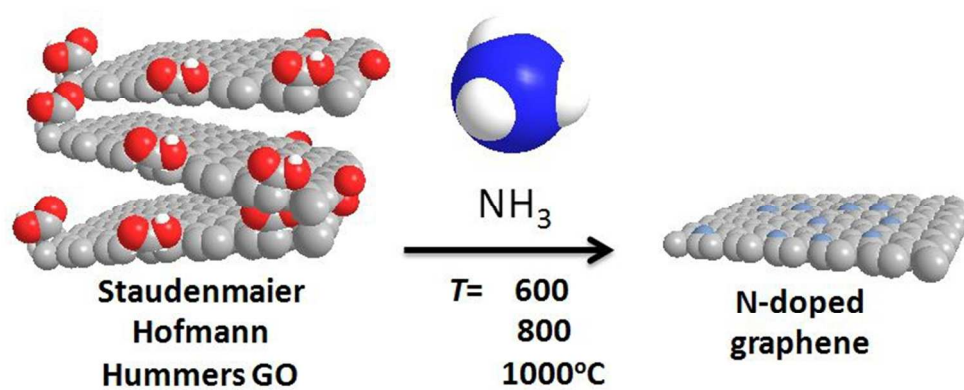
1 C.N.R. Rao, A.K. Sood, K.S. subrahmanyam, A. Govindaraj, *Angew. Chem. Int. Ed.* 2009, **48**, 7752.

2 L. S. Panchakarla, K. S. Subrahmanyam, S. K. Saha, A. Govindaraj, H. R. Krishnamurthy, U. V. Waghmare, and C. N. R. Rao, *Adv. Mater.* 2009, **21**, 4726.

3 Z.S. Wu, W. Ren, L. Xu, F. Li, H.M. Cheng, *ACS Nano*, 2011, **5**, 5463.

-
- 4 Z. Jin, J. Yao, C. Kittrell and J. M. Tour, *ACS Nano*, 2011, **5**, 4112.
- 5 L. Qu, Y. Liu, J.-B. Baek and L. Dai, *ACS Nano*, 2010, **4**, 1321.
- 6 A. L. M. Reddy, A. Srivastava, S. R. Gowda, H. Gullapalli, M. Dubey and P. M. Ajayan, *ACS Nano*, 2010, **4**, 6337.
- 7 X. L. Gou, R. Li, Z. D. Wei and W. Xu, *RSC Adv*, 2013, **3**, 9978.
- 8 Hwee Ling Poh, Petr Simek, Zdenek Sofer, Martin Pumera, *ACS Nano*, 2013, **7**, 5262.
- 9 F. Karlicky, K.K.R. Datta, M.Otyepka, and R. Zboril, *ACS Nano*, 2013, **7**, 6434.
- 10 H. L. Poh, P. Simek, Z. Sofer, M. Pumera, *Chem. Eur. J.* 2013, **19**, 2655.
- 11 D. C. Elias, R. R. Nair, T. M. G. Mohiuddin, S. V. Morozov, P. Blake, M. P. Halsall, A. C. Ferrari, D. W. Boukhvalov, M. I. Katsnelson, A. K. Geim, K. S. Novoselov, *Science*, 2009, **323**, 610.
- 12 A. Y. S. Eng, H. L. Poh, F. Šaněk, M. Maryško, S. Matějková, Z. Sofer, M. Pumera, *ACS Nano*, 2013, **7**, 5930.
- 13 L.S. Zhang, X.Q. Liang, W.G. Song, Z.Y. Wu, *Phys Chem Chem Phys*, 2010, **12**, 12055.
- 14 H.M. Jeong, J.W. Lee, W.H. Shin, Y.J. Choi, H.J. Shin, J.K. Kang, J.W. Choi, *Nano Lett*, 2011, **11**, 2472.
- 15 F.B. Wang, Z.H. Sheng, L. Shao, J.J. Chen, W.J. Bao, X.H. Xia, *ACS Nano*, 2011, **5**, 4350.
- 16 H. L. Poh, P. Simek, Z. Sofer, I. Tomandl, M. Pumera, *J. Mater. Chem. A*, 2013, **1**, 13146.
- 17 Y. Zheng, Y. Jiao, L. Ge, M. Jaroniec, and S.Z. Qiao, *Angew. Chem. Int. Ed.* 2013, **52**, 3110.
- 18 D.W. Chang, E.K. Lee, E.Y. Park, H. Yu, H.J. Choi, I.Y. Jeon, G.J. Sohn, D. Shin, N. Park, J.H. Oh, L. Dai, J.B. Baek, *J. Am. Chem. Soc.* 2013, **135**, 8981.
- 19 C. K. Chua, Z. Sofer, M. Pumera, *Chem. Eur. J.* 2012, **18**, 13453.
- 20 L. Staudenmaier, *Ber. Dtsch. Chem. Ges.* 1898, **31**, 1481.
- 21 U. Hofmann, E. Konig, *Z. Anorg. Allg. Chem.* 1937, **234**, 311.
- 22 W. S. Hummers, R. E. Offeman, *J. Am. Chem. Soc.* 1958, **80**, 1339.
- 23 Z. Sofer, P. Simek, M. Pumera, *Phys. Chem. Chem. Phys.* 2013, **15**, 9257.
- 24 H.L. Poh, F. Sanek, A. Ambrosi, G. Zhao, Z. Sofer, M. Pumera, *Nanoscale*, 2012, **4**, 3515.
- 25 L. G. Cançado, K. Takai, T. Enoki, M. Endo, Y. A. Kim, H. Mizusaki, A. Jorio, L. N. Coelho, R. Magalhaes-Paniago, M. A. Pimenta, *Appl. Phys. Lett.* 2006, **88**, 163106.
- 26 L. J. Van der Pauw, *Philips Res. Rep.*, 1958, **13**, 1.
-

Level of nitrogen doping of graphene strongly depends on type of the starting graphite oxide and temperature used.



173x74mm (120 x 120 DPI)